JOURNAL OF CATALYSIS 76, 393–404 (1982)

# Deactivation Characteristics of an Acrolein Oxidation Catalyst

## II. Kinetics of Crystallization

PETER B. DEGROOT AND LEON B. LEVY

*Celanese Chemical Company Technical Center, Post Office Box 9077, Corpus Christi, Texas 78408*

Received October 23, 1981; revised March 5, 1982

A high-temperature, controlled-atmosphere X-ray diffractometer was used to measure rates of crystallization of a mixed metal molybdate catalyst. The catalyst, initially amorphous, becomes crystalline at temperatures of 400–500°C. This occurs slowly in inert atmospheres and much more rapidly in air. After thermal treatment in air, relative acrolein oxidation activity is proportional to the fraction of the catalyst which remains uncrystallized. The phases observed in air include $V_2O_5$, $MnMoO_4$, and $MoO_3$. The phases crystallizing in inert atmospheres are $MnMoO_4$, $Mo_4O_{11}$, $W_{18}O_{49}$, and $V_4O_9$. Unidentified phases remain in both cases. Crystallization follows a second-order rate law, with a rate constant of $7 \times 10^{-3}$ hr$^{-1}$ in dry air at 410°C. Water vapor in air, even at 10–20 ppm, increased the rate markedly. In inert atmospheres, $H_2O$ has no effect. The initially active catalyst probably contains compounds similar to molybdenum shear structures. Crystallization in air proceeds by an annealing out of oxygen vacancy defects and subsequent crystal growth.

## INTRODUCTION

This study was undertaken to relate physical or chemical characteristics of an acrolein oxidation catalyst to changes in activity occurring with time, temperature, and atmosphere. The Mo–V–W–Mn oxide catalysts, and the kinetics of deactivation, have been described in Part I of this paper (*1*).

Earlier studies in this laboratory of the calcination of similar catalysts at different temperatures indicated that significant changes in the X-ray diffraction (XRD) pattern occurred with increasing temperature of calcination. Other analyses, including infrared spectroscopy, X-ray photoelectron spectroscopy, mercury porosimetry, thermogravimetric analysis, and scanning electron microscopy examination coupled with X-ray fluorescence microanalysis failed to reveal any temperature-related effects as dramatic as those in the XRD spectrum.

The series of experiments performed followed two different paths. One approach was to examine, by XRD, materials that had actually undergone deactivation kinetic experiments as described in the previous paper (*1*). Analysis of these data provided a direct correlation between activity and crystal phase properties. The second approach was to examine a catalyst sample by XRD *in situ* while it was undergoing thermal treatment paralleling that in the deactivation kinetic experiments. These XRD kinetic experiments provided a nearly continuous record of the transformations occurring under conditions of catalyst deactivation, and thus gave insight into the details of this process.

## METHODS

*Catalyst.* The catalyst composition and general method of preparation have been described previously (*1*). Catalyst I was calcined at a temperature of 385°C and catalyst II at 320°C. All catalyst samples were ground to −100 mesh (<0.15 mm) before X-ray diffraction analysis.



0021-9517/82/080393-12$02.00/0

*Diffractometer.* A Philips X-ray diffractometer equipped with a graphite crystal monochrometer was used to collect XRD data. The radiation used was Cu $K\alpha$. A Tracor Northern NS 880 X-ray fluorescence data system was interfaced with the diffractometer to automate data acquisition and reduction. Portions of the XRD powder diffraction spectrum were scanned repetitively, and the intensity-time data stored on magnetic tape.

A Materials Research Corporation Model X-86-N3 high-temperature-controlled-atmosphere diffraction chamber was used to allow analysis of the catalyst under different atmosphere and temperature conditions. Samples were ground, slurried with isopropanol, and transferred to the sample stage. The solvent was then allowed to evaporate. A controlled thickness of sample on the sample stage was obtained by using 10 $\mu$l of a slurry of 2.0 g of catalyst in 3.0 ml of isopropanol. This amount gave a sample thickness of about 0.1 mm.

*Sample atmosphere.* A manifold system for introducing various gases into the sample chamber was constructed. Air was provided either from the laboratory compressed air supply or from bottled air. Both "industrial" and "zero" grade bottled air were employed. The nitrogen used was obtained from boil-off of liquid nitrogen. In some experiments, the gases were dried by passing them through a $P_2O_5$ drying tube before being introduced into the chamber. In other experiments, the gases were saturated with water vapor (at ambient temperature) by passing them through a fritted glass bubbler containing distilled water. Gas flow rates ranged from about 200 to about 900 $cm^3$/min. Pressure in all cases was atmospheric pressure.

*Sample temperature.* The temperature of the sample was measured using a Pt/Rh thermocouple welded to the bottom of the heated sample stage. Thermocouple readings were obtained on a Thermoelectric Minimite model thermocouple bridge. The sample stage thermocouple was calibrated by observing the disappearance of the X-ray diffraction pattern of powdered zinc at the melting point (419.5°C). Temperature could generally be maintained to within ±2°C of the set temperature over a period of several days.

## RESULTS AND DISCUSSION

### *Initial State of Catalyst*

In catalysts calcined at or below calcination temperatures of about 385°C, the X-ray diffraction spectrum is nearly featureless, indicating an essentially amorphous material. There are two rather diffuse peaks, one at about 22° $2\theta$ and a broad feature from about 25 to 30° $2\theta$. The initial spectrum in Fig. 1 illustrates this for catalyst II calcined at 320°C. These peaks are somewhat sharper for catalyst I, calcined at 385°C. The catalyst calcined at the higher temperature has a surface area of 9.1 $m^2$/g while that of the catalyst calcined at the lower temperature is 15.8 $m^2$/g.

### *Development of Crystallinity*

It was known that calcination at too high a temperature in air would cause development of peaks in the X-ray powder diffraction spectrum. For example, heating a sample in air to about 430°C overnight would develop a very distinct crystalline XRD pattern. However, it was discovered that heating a sample of the same catalyst overnight at the same temperature in nitrogen produced absolutely no development of crystallinity. Subsequent experiments showed that crystallinity could be developed in an inert atmosphere, but only if the temperatures were considerably higher. Moreover, the X-ray diffraction patterns developed in air and in nitrogen are quite different (Fig. 2).

### *Identification of Crystalline Phases*

Figure 3 shows the spectrum of a sample of catalyst I which had been exposed to air at 410°C for 96 hr. At this point, crystallization is essentially complete. As can be seen,

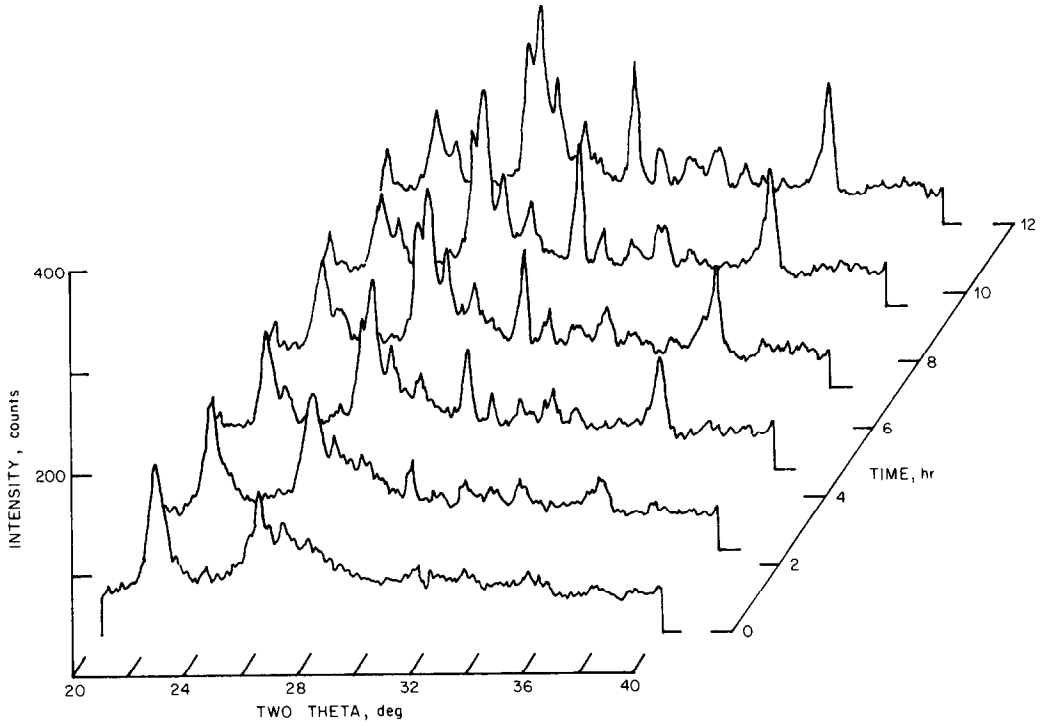


FIG. 1. Crystallization of catalyst II at 410°C in air containing 2.8 vol% $H_2O$. Time shown is at start of $2\theta$ scan: scan rate 1 deg/min.

the spectrum is very complex, with about 60 statistically significant peaks in the 6 to 66° $2\theta$ range.

Figure 3 also shows the powder diffraction patterns of the four crystalline phases considered to be the best match to the major peaks observed in the catalyst spectrum. Both manual searching techniques and the search/match computer program of the Joint Committee on Powder Diffraction Standards (JCPDS) were used to screen possible pattern matches. $V_2O_5$, $MnMoO_4$, and $MoO_3$ are probably all present, although the match for some of the peaks in these phases is not exact. One can rationalize these slight mismatches by invoking peak shifts and intensity variations caused by the formation of solid solutions and perhaps partial substitution of one metal for another in the oxide phases. The presence of $Mn_2O_3$ is questionable, but it is the only phase found which accounts reasonably well for the fairly intense peak at about 36° $2\theta$. However, the phases identified do not account for a number of relatively large peaks remaining in the spectrum, and none of the phases identified contained any tungsten.

The spectrum of a catalyst I sample which had been treated at 450°C in $N_2$ for a sufficient time to develop complete crystallinity is shown in Fig. 4. The patterns of several compounds considered to be present are also shown. These patterns were matched by similar techniques to those described above.

The crystal phases resulting from thermal treatment in an inert atmosphere are quite different from those produced in air. The only phase which appears to be common to the two materials is $MnMoO_4$. The other two compounds whose diffraction patterns match portions of the unknown pattern quite well are two different crystal forms of $Mo_4O_{11}$. Two other compounds are possibly present in rather low concentrations. They

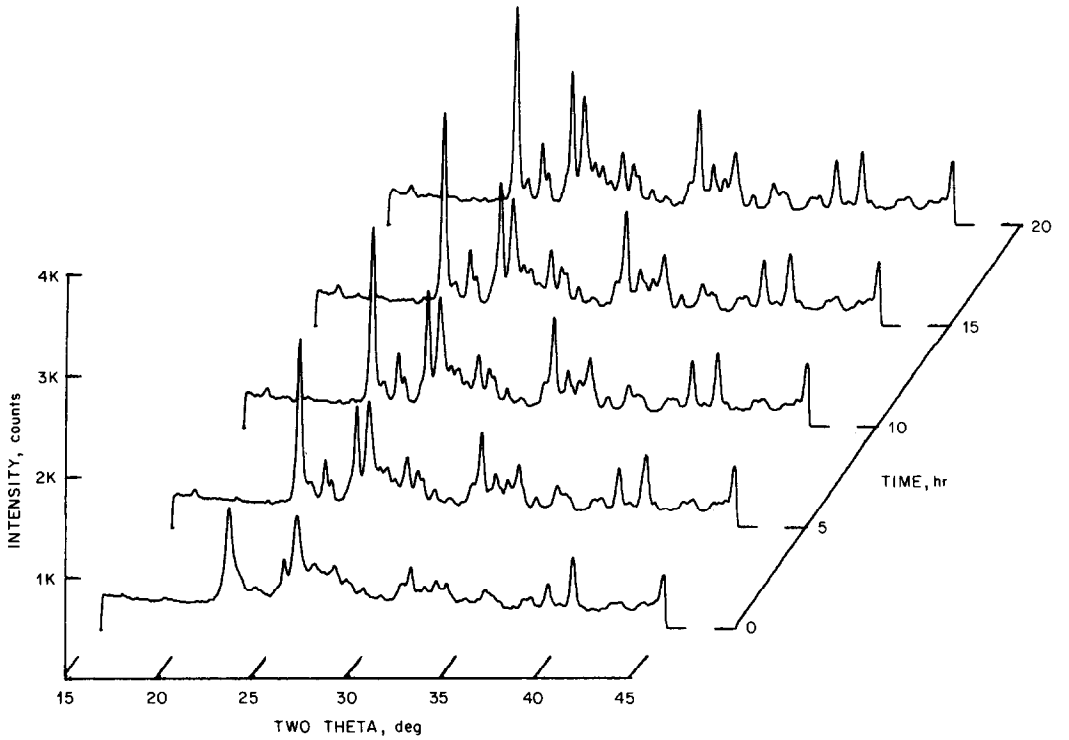


FIG. 2. Crystallization of catalyst I at 450°C in $N_2$. Time shown is at start of $2\theta$ scan: scan rate 1/4 deg/min. Peak at about 40° $2\theta$ is from Pt/Rh sample stage.

are $W_{18}O_{49}$ and $V_4O_9$. Some mismatches in the fit of these last two patterns may be rationalized in the same manner as the mismatched lines in the spectrum of the air-treated catalyst spectrum discussed above. More than half of the catalyst diffraction pattern intensity remains unaccounted for. In particular, a great portion of the intensity of the major peaks in the spectrum at about 22° $2\theta$ remains unaccounted for.

Steps were taken to ensure that preferential orientation of the crystals did not distort the diffraction patterns sufficiently to cause difficulties with identification of the crystalline constituents. The XRD spectrum obtained from material which had been removed, reground, and run in a conventional sample holder was essentially the same as that obtained on the hot stage of the controlled-atmosphere diffractometer attachment.

*Crystallization and Oxidation State*

In general terms, the samples treated in air and $N_2$ differ in the oxidation state of the metals in the oxides present. Those phases that could be identified in the air-treated sample are in the highest oxidation state, while all but one compound identified in the $N_2$-treated material are somewhat oxygen-deficient. $Mo_4O_{11}$ and $V_4O_9$ belong to a class of compounds which include the well-known "shear structures" (*2–6*). $W_{18}O_{49}$ is related to the tungsten bronzes, and to "tunnel" structures such as $Mo_{17}O_{47}$ (*7–12*). Although often called "nonstoichiometric," all of these compounds are definite stoichiometric compositions in which the "missing" oxygen is accommodated by a periodic modification of the lattice. In the simple shear structures (tungsten and molybdenum compounds of the type

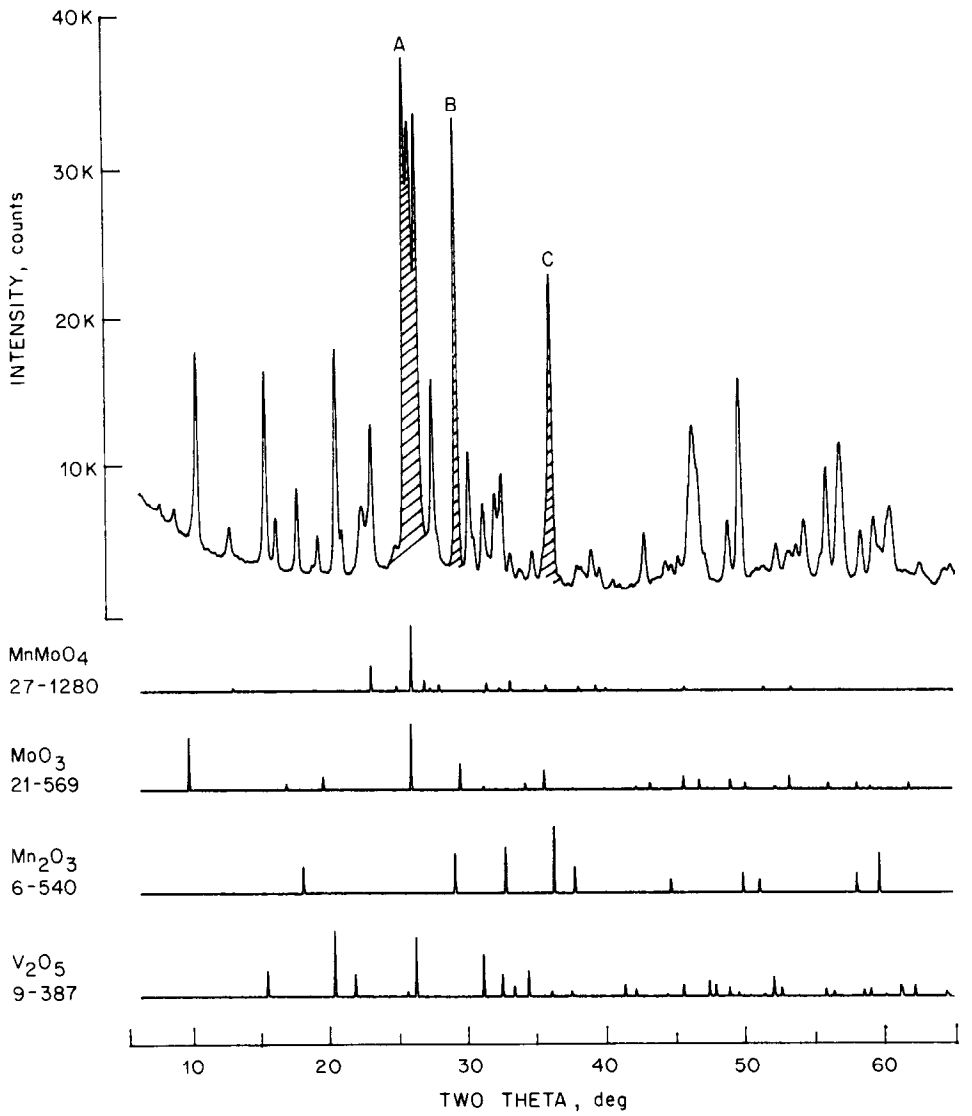


FIG. 3. XRD spectrum of catalyst I after 96 hr in air at 410°C. Patterns of phases shown are the best matches found. Numbers given are JCPDS data file numbers.

$M_nO_{3n-1}$), the decreased number of oxygens are accommodated by a change from corner-sharing between $MO_6$ octahedra to edge-sharing at certain lattice positions. More complicated structures can involve a change from corner to edge-sharing, a change of some structural units from octahedra to other polyhedra, or both.

The results suggest that the catalyst consists of a mixture of amorphous compounds which include some oxygen-deficient phases. It could be argued that oxygen-deficient amorphous phases are not present initially and that the thermal treatment under nitrogen causes loss of oxygen and development of these phases. This does not seem likely, since reported formation temperatures for these compounds by reduction or decomposition of the parent oxide generally are 100°C or more higher than the present case (*14*, *15*).

As discussed in Part I of this work (*1*),

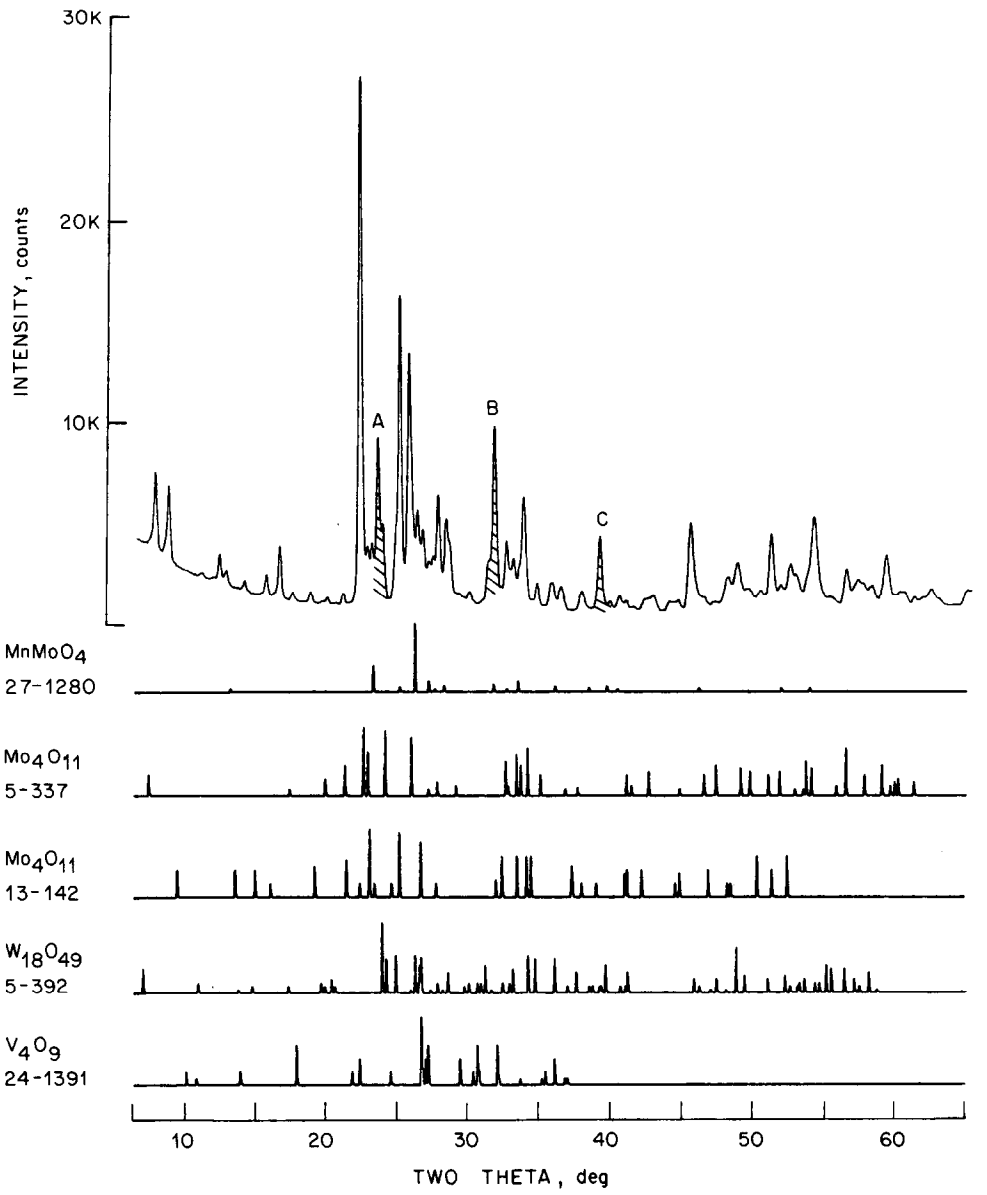


FIG. 4. XRD spectrum of catalyst I after 16 hr in $N_2$ at 450°C. Patterns shown are the best matches found. Numbers given are JCPDS data file numbers.

these reduced phases may be the catalytically important species. A facile reduction and reoxidation of the catalyst has been suggested as necessary for acrolein oxidation (*13*).

From the difference in catalyst behavior when heated in air compared to an inert atmosphere, it appears that the phenomenon observed as "crystallization" involves oxidation. Oxidation state may well be the property fundamentally related to activity, although one might also expect some decrease in activity due simply to loss of surface area as crystal growth occurs. One other observation supporting this view is from a single experiment in which activity

of a catalyst which crystallized in $N_2$ was measured. Although the relative crystallinity had reached about 0.5, the relative activity remained about 0.9 of that of a fresh catalyst. However, since crystallinity is the observable variable in these experiments the kinetics will be discussed in terms of crystallization rate.

*Crystallization Rate of Different Phases*

It was observed in both air (Fig. 1) and nitrogen (Fig. 2) experiments that virtually all the peaks in each spectrum grew at about the same rate. This was very surprising. One might reasonably expect that the different compounds present would crystallize at different rates. The similar crystallization rates suggest that the rate-limiting step may be the decomposition or oxidation of a single precursor compound or solid solution. Alternatively, the initial crystallization of one phase may act as a nucleation site for the crystallization of the other phases present in an intimately mixed amorphous solid.

*Quantitative Measurement of Crystallinity*

Three strong characteristic peaks in both the air/thermal treatment and nitrogen/thermal treatment spectra were selected to be used to follow the kinetics of crystallization in these two atmospheres. The peaks selected are shown as regions A, B, and C in Figs. 3 and 4. In two cases, the regions selected are multiple overlapping peaks rather than single peaks. As all these peaks were observed to grow at the same rate, this should introduce no complications. Likewise, the fact that the selected peaks do not correspond to identified single phases should be of no consequence.

Peak areas were measured for each spectrum in each of the three areas of interest. Background was subtracted from peak area by a linear extrapolation of average background measured in regions 0.3° $2\theta$ wide on either side of the peak. The precision of measurement of the peak areas was ±5 to 10%. It was limited both by the stability of the X-ray equipment and the statistics of measuring small peaks at the beginning of the experiment.

Peak intensities were converted to a quantitative dimensionless measure of crystallinity. The relative degree of crystallinity, $X_c$, was set equal to $(I - I_0)/(I_\infty - I_0)$, where $I_0$ is the intensity, if any, in the region of interest at the start of an experiment, and $I_\infty$ is the intensity in the region of interest when crystallization is essentially complete.

*Relationship of Crystallinity to Activity*

To investigate the connection between catalytic activity and crystallinity, two experiments were set up with the use of a sufficiently large quantity of catalyst in the fixed-bed reactor so that small samples could be removed after different lengths of time for XRD analysis. These deactivation experiments were two of those described in the preceding part of this investigation (*1*).

The working hypothesis of these experiments was that activity was directly related to the concentration of some amorphous phase, or proportional to one minus the fraction of the sample that is crystalline. If this is correct, a plot of one minus the relative activity vs the relative crystallinity should be linear with a slope of 1 and should pass through the origin. As shown in Fig. 5, the data fit the proposed relationship quite well.

*Crystallization Kinetics in Air*

The kinetic behavior of catalyst samples in air and air–water vapor mixtures was investigated by following the increase in the selected XRD peak areas as a function of time. In general, the conditions under which crystallization kinetics were obtained paralleled those employed in the fixed-bed reactor deactivation kinetic study described previously (*1*). Crystallization rates were also treated similarly to deactivation rates. An apparent rate constant, $k_a$, at constant oxygen and water vapor partial pressure was defined to determine the ki-

netic order of the crystallization rate, i.e.,

$$\frac{dX_c}{dt} = k_a(1 - X_c)^n.$$

The results of a typical crystallization kinetic experiment are shown in Fig. 6. The scatter in the data reflects the precision of peak area measurements obtainable with this X-ray diffraction system. As a result of this scatter, it is not possible to distinguish between overall first- or second-order dependence of crystallinity on $X_c$. Calculations of the apparent rate constant by the method of least-squares yield a correlation coefficient which is about the same for either first- or second-order kinetics and is between 0.90 and 0.97 for all of the experiments. This is true whether the data are weighted or not. Weighting of the data insures that a point at large $X$ value (long time) will not have an unjustifiably large effect on the slope and, hence, on the rate. The weighting used assumes a constant variance $dV$ in the measured variable $V$ and propagates this variance through the appropriate kinetic equation to obtain $d[f(V)]$. Measured variables are then weighted by $W = 1/[d(f(V)]^2$.

Several pretreatments of the catalysts before commencing the kinetic experiments were also tried. These were designed to bring the catalyst surface to its equilibrium hydration state so that any slow equilibration which might occur would not affect the initial kinetic points. These pretreatments consisted of flowing dry nitrogen or nitrogen plus water vapor at the temperature of the experiment for 15 to 50 min before introducing the test atmosphere. In one case, the pretreatment consisted of dry air at a temperature low enough so that no significant crystallization would take place and in one other case, the pretreatment consisted of water vapor and nitrogen at room temperature.

Results of the kinetic experiments, along with details of the experimental conditions, are given in Table 1. The rate-enhancing ef-

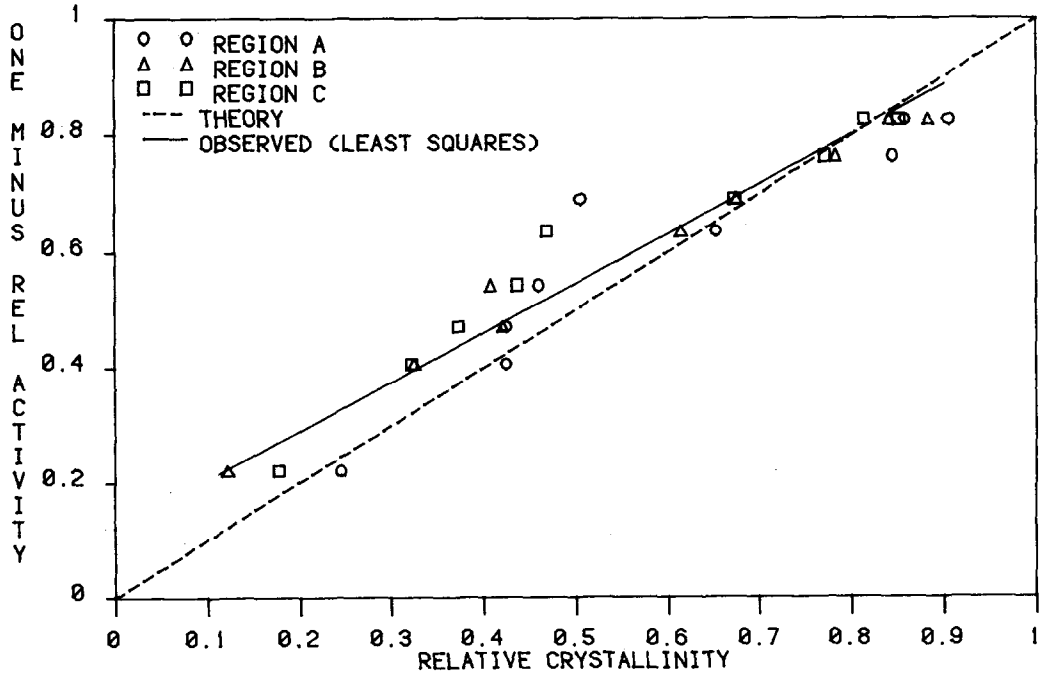


FIG. 5. Correlation between relative activity of catalyst for acrolein oxidation and relative crystallinity.

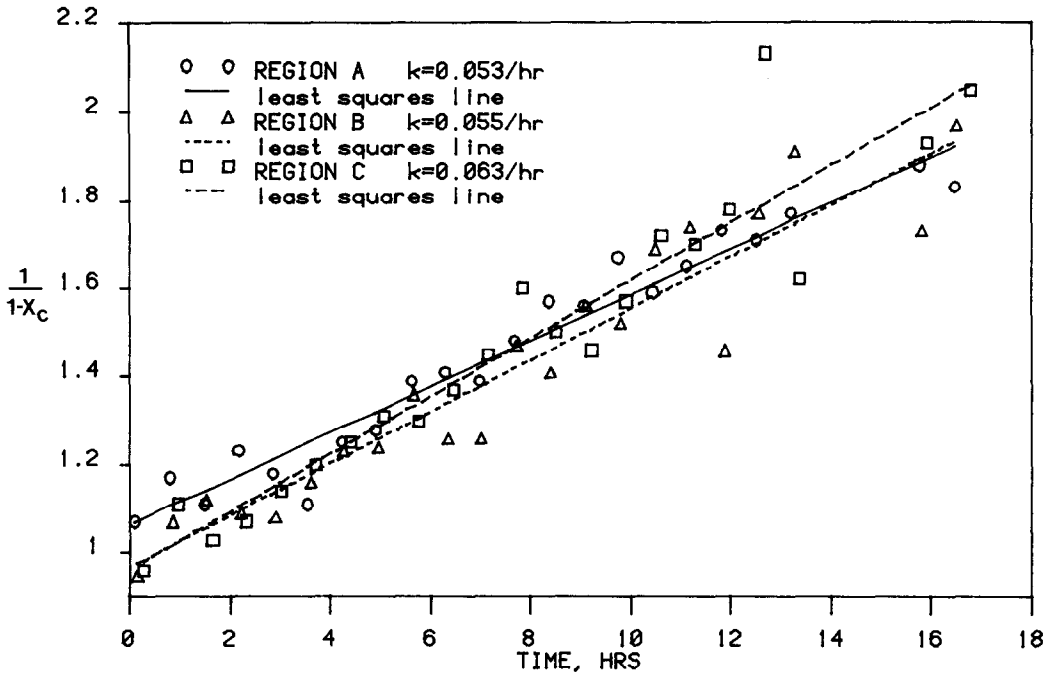


FIG. 6. Second-order kinetic plot of data from thermal treatment of catalyst I in air + 2.8 vol% $H_2O$ at 410°C. Second-order effective rate constants from slope calculated by method of least-squares.

fect of water vapor in the atmosphere can readily be seen from the experiments with catalyst I (normal 385°C calcination). Even the amount of water vapor present in industrial grade cylinder air (10 to 20 ppm) increases the rate constant by nearly an order

TABLE 1

Rate of Catalyst Crystallization in Air and Air/Water Vapor Atmosphere

| Catalyst | Pretreatment | Atmosphere | Temperature (°C) | $k_a \times 10^2$ $hr^{-1}$ [a] |
|---|---|---|---|---|
| I | None | Air[b] | 410 | 9.6 |
| | None | Air, dried[d] | 410–414[d] | 1.2 |
| | None | Air[b] | 410 | 6.3 |
| | None | Air, dried[c] | 410 | 0.82 |
| | Air, dried; 200°C, 40 min | Air, dried[c] | 410 | 0.59 |
| | $N_2$, dried; 410°C, 50 min | Air[b] | 410 | 3.3 |
| | None | Air + 2.8 mol%, $H_2O$ | 410 | 5.7 |
| | $N_2$ + 2.8 mol% $H_2O$; 23°C, 35 min | Air + 2.8 mol%, $H_2O$ | 410 | 5.6 |
| | $N_2$, dried; 410°C, 35 min | Air, dried | 410 | 0.70 |
| | $N_2$ + 2.8 mol% $H_2O$; 433°C, 15 min | Air + 2.8 mol%, $H_2O$ | 433 | 51 |
| II | $N_2$ + 2.8 mol% $H_2O$; 410°C, 25 min | Air + 2.8 mol%, $H_2O$ | 410 | 10 |
| | $N_2$ + 2.8 mol% $H_2O$; 410°C, 25 min | Air + 2.8 mol%, $H_2O$ | 410 | 8.3 |
| | $N_2$, dried; 410°C, 25 min | Air, dried | 410 | 3.3 |

[a] Second-order effective rate constant.
[b] Cylinder air, industrial grade.
[c] Dried by passing through $P_2O_5$.
[d] Temperature drifted from 410°C at beginning of experiment to 414°C at end.

of magnitude. The second-order rate constant in $P_2O_5$-dried air, with or without catalyst predrying, ranges from $6 \times 10^{-3}$ to $8 \times 10^{-3}$ $hr^{-1}$ at 410°C, while the rates from two different cylinders of industrial air are about $6 \times 10^{-2}$ and $1 \times 10^{-1}$. A drying pretreatment seems to have little effect on the rate in dry air but a drying pretreatment reduces the observed rate for cylinder air by about a factor of 2. Apparently, dehydration of the surface is fast, but in air containing only low concentrations of water vapor, there is a relatively slow rehydration of a dried catalyst surface. In experiments with high concentrations of water vapor (2.8 mol%), rehydration of the surface is faster and pretreatment has little effect on the kinetics.

A comparison of the results of cylinder air with air containing 2.8% $H_2O$ also suggests that the crystallization process, at least under these experimental conditions, does not follow a simple first- or second-order dependence on water vapor concentration. That is, small changes in water vapor concentration at very low concentration levels have profound effects and the effect rapidly diminishes for higher water vapor concentrations. This would be consistent with Langmuir–Hinshelwood-type rate expressions as proposed in the preceding paper (*1*).

Some interesting effects of calcination temperature were also observed. As shown in Table 2, the initial rate of crystallization at 410°C for catalyst II (calcined at 320°C) is about six to eight times greater than for catalyst I (calcined at 385°C) in dry air. In the latter stages of crystallization, the rate drops to about a factor of 2 to 3 greater than with catalyst I. In air plus water vapor, the crystallization rate for catalyst II is greater than that for catalyst I by a factor of about 2. For catalyst II in an air/water vapor atmosphere, the initial rate is essentially the same as the overall rate and no curvature of the second-order rate plot is apparent. Since the kinetic experiments are done at a temperature somewhat above the normal calcination temperature, presumably catalyst II is not only going through the air/water vapor-induced crystallization but is also, in effect, being calcined during the initial stages of the kinetic experiments.

TABLE 2

Dependence of Crystallization Rate on Calcination Temperature of Catalyst

| Catalyst | Calc. temp. (°C) | $k_a \times 10^2$, $hr^{-1}$ [a] at 410°C | |
|---|---|---|---|
| | | In dry air | In air + 2.8 mol% $H_2O$ |
| I | 385 | 0.82 | 5.7 |
| | | 0.59 | 5.6 |
| | | 0.70 | |
| II | 320 | 5.2[b] | 11[b] |
| | | 1.8[c] | 10[c] |
| | | | 8.0[b] |
| | | | 8.3[c] |

[a] Second order effective rate constant.
[b] Initial rate during first 3–4 hr.
[c] Final rate, time >36 hr.

These results suggest that one of the things that may be occurring during calcination in the temperature interval 320–385°C may be loss of some very tightly bound water or hydroxyl groups, which, when present, catalyze crystallization of the catalyst.

Two other facts pertaining to the presence of water vapor in the atmosphere should be noted. First, the effect of water vapor is only present when air is also present. Water vapor in nitrogen has no effect on the rate of crystallization. The second point is that the same X-ray diffraction pattern evolves either in the absence or presence of water vapor, at least up to the 2.8% water vapor level investigated here.

### *Differences between Crystallization and Deactivation Kinetics*

Qualitatively, the effects of air and water vapor on crystallization and on deactivation are the same. Moreover, a good correlation between degree of crystallinity and loss of

activity was described earlier. However, there appear to be some differences in details of the kinetic behavior between the deactivation kinetic experiments in the fixed-bed reactor (*1*) and the XRD kinetic experiments. There is a very large difference in the value of the second-order rate constant in dry air at 410°C in the two cases. For catalyst I, in an atmosphere of dry air, the average value of the second order effective rate constant, $K_a$, from the XRD experiments is about $7 \times 10^{-3}$ $hr^{-1}$. For the deactivation experiments under these same conditions, the value of $K_a$ is about $1.3 \times 10^{-1}$ or nearly 20 times larger.

In wet air, the discrepancy is somewhat smaller. Here, the rate of crystallization is about a factor of 10 greater than the deactivation rate in the fixed-bed reactor studies. Using the rate equation given in Part I (*1*), the deactivation rate with 2.8% $H_2O$ in air is 0.5 $hr^{-1}$ while the crystallization rate observed under these conditions is 0.06 $hr^{-1}$.

Considerable effort was expended in ensuring that no differences in temperature or air source were present which could cause the observed differences in rates. There remains, however, an unavoidable difference in the physical form of the catalyst in the two experiments. We feel that diffusion effects within the catalyst particles may be responsible for the rate discrepancies, and is related to differences in the particle size in the two types of experiments. In the XRD experiments, the catalyst is cast as a very thin (~0.1 mm) film of very fine (<0.15 mm diameter) powder particles. In the deactivation kinetic experiments the catalyst is present as 20–30 mesh (~0.7 mm diameter) particles. In addition, it was observed that a controlled thickness of sample on the heated sample stage of the XRD equipment was necessary to obtain reproducible kinetic results.

### *Mechanism of Crystallization*

Because of the dependence of crystallization rate on oxygen, it seems likely that this process involves the annealing of an oxygen-deficient phase similar to the well-known molybdenum shear structures. Thermogravimetric analysis (TGA) did not measure any uptake of oxygen in the temperature range of interest, but the oxygen vacancy concentration may be too low to measure by our instrumentation. It may be that the initial state of the catalyst is not that of an extensive oxygen-deficient structure but rather that of a few small areas of disorder or oxygen deficiency. It might be noted that TGA experiments in inert atmospheres did not detect any weight *loss*, either.

Mechanistically, the role of water vapor at the very low concentrations at which it has a noticeable effect, is difficult to imagine, although some possibilities were advanced in Part I (*1*). Alternatively, perhaps a hydroxylated surface of some sort enhances the adsorption of the oxygen prior to its subsequent migration into the lattice to combine with oxygen vacancy defects. Such enhanced oxygen adsorption has been reported for oxides of Al, Si, Ti, and Cr (*16*).

There is very little information in the literature on redox properties of phases similar to those found in this catalyst, especially with regard to the effect of water vapor. Kihlborg (*14*) did investigate the reoxidation of some of the molybdenum oxygen-defect compounds in ambient air, which presumably contained considerable water vapor, in the temperature range 230–350°C. He reported that orthorhombic $Mo_4O_{11}$ was oxidized the most rapidly, being completely transformed to $MoO_3$ within 18 hr at about 300°C. Adsorbed surface water was found to play an essential role in the transport of the reducing species during the reduction of $WO_3$ by hydrogen (*17*). Batist *et al.* (*18*) observed during butene reduction of several nonstoichiometric molybdenum oxides, including $Mo_4O_{11}$, that all of these oxides except $Mo_{17}O_{47}$ showed an induction period, after which the reduction rate increased markedly. It is possible that this

rapid increase in reduction rate is due to the accumulation and adsorption of water produced from the initial slow reaction of the butene with the oxide.

*Applications to Other Catalyst Studies*

The results of these parallel kinetic investigations of catalyst deactivation and development of crystallinity have some implications for catalyst research on other similar catalysts. Defect molybdate, tungstate, or vanadate structures are thought to be involved in many selective oxidation catalysts (*19*). Part of the catalytic mechanism, the reoxidation or replacement of lattice oxygen in the catalyst, is also thought to depend on the mobility of lattice oxygen in the structure. The methods developed here allow these kinds of effects to be investigated conveniently. In addition, they may also lead to an understanding of the relationship of preparation and calcination conditions to the initial activity and subsequent deactivation rate of the catalyst under selected conditions.

The results presented here also suggest that the composition, structure, and properties of the amorphous phase of the catalyst are really what is of interest. As noted in the Introduction, a few methods (infrared spectroscopy, X-ray photoelectron spectroscopy, and others) which can give information on noncrystalline states, yielded no useful information in the present case. However, other methods such as Raman spectroscopy and high-resolution electron beam diffraction techniques certainly might reveal a more fundamental relationship between catalyst structure and performance.

ACKNOWLEDGMENTS

We wish to thank G. W. Keulks and G. L. Schrader for interesting and helpful discussions of the possible role of molybdate shear structures. We also thank C. C. Hobbs for helpful suggestions on statistical weighting of kinetic data.

REFERENCES

1. Levy, L. B., and DeGroot, P. B., *J. Catal.* **76,** 385 (1982).
2. Kihlborg, L., *in* "Advances in Chemistry Series, 39," pp. 37–45. American Chemical Society, Washington, 1963.
3. Wadsley, A. D., *Rev. Pure Appl. Chem. (Aust.)* **5,** 165 (1955).
4. Magneli, A., *Acta Chem. Scand.* **7,** 315 (1953).
5. Magneli, A., *Arkiv Kemi* **1,** 213 (1949).
6. Magneli, A., *Arkiv Kemi* **1,** 269 (1949).
7. Andersson, S., and Jahnberg, L., *Arkiv Kemi* **21,** 413 (1963).
8. Blomberg, B., Kihlborg, L., and Magneli, A., *Arkiv Kemi* **6,** 133 (1953).
9. Magneli, A., Blomberg-Hansson, B., Kihlborg, L., and Sundkvist, G., *Acta Chem. Scand.* **9,** 1382 (1955).
10. Israelsson, M., and Kihlborg, L., *Arkiv Kemi* **30,** 129 (1968).
11. Pailleret, P., Borensztajn, J., Freundlich, W., and Rimsky, A., *C. R. Acad. Sci. (Paris) C* **263,** 1131 (1966).
12. Magneli, A., *Acta Crystallogr.* **6,** 495 (1953).
13. Novakova, J., Jiru, P., and Zavadil, V., *Coll. Czech. Chem. Commun.* **37,** 1233 (1972).
14. Kihlborg, L., *Acta Chem. Scand.* **13,** 954 (1959).
15. Kihlborg, L., and Magneli, A., *Acta Chem. Scand.* **9,** 471 (1955).
16. Ponec, V., Knov, Z., and Cerny, S., "Adsorption on Solids," pp. 447–448. CRC Press, Cleveland, 1965.
17. Boudart, M., Vannice, M. A., and Benson, J. E., *Z. Phys. Chem. Neue Fol.* **64,** 171–77 (1969).
18. Batist, Ph. A., Kapteijens, C. J., Lippens, B. C., and Schuit, G. C. A., *J. Catal.* **7,** 33 (1967).
19. Haber, J., and Witko, M., *Acc. Chem. Res.* **14,** (1981).